Measurement-based Evaluation of the Impact of Large Vehicle Shadowing on V2X Communications

Rodriguez, Ignacio; Portela Lopes de Almeida, Erika; Lauridsen, Mads; Assefa, Dereje; Gimenez, Lucas Chavarria; Nguyen, Huan Cong; Sørensen, Troels Bundgaard; Mogensen, Preben Elgaard

Published in:
European Wireless 2016; 22th European Wireless Conference

Publication date:
2016

Document Version
Publisher's PDF, also known as Version of record

Measurement-based Evaluation of the Impact of Large Vehicle Shadowing on V2X Communications

Ignacio Rodriguez[1], Erika P. L. Almeida[1,2], Mads Lauridsen[1], Dereje A. Wassie[1], Lucas Chavarria Gimenez[1], Huan C. Nguyen[1], Troels B. Sørensen[1], and Preben Mogensen[1,3]

[1]Department of Electronic Systems, Aalborg University, Denmark.
[2]Instituto de Desenvolvimento Tecnológico (INDT), Manaus/Brasília, Brazil.
[3]Nokia - Bell Labs, Research Center Aalborg, Denmark.

Emails: {irl,eplda,ml,daw,lcg,hcn,tbs,pm}@es.aau.dk

***Abstract*—Upcoming applications, such as autonomous vehicles, will pose strict requirements on the vehicular networks. In order to provide these new services reliably, an accurate understanding of propagation in the vehicular scenarios is needed. In this context, this paper presents a measurement-based evaluation of large vehicle shadowing at 5.8 GHz in V2X scenarios. The receiver antenna height is fixed to average vehicular height (1.5 m), while the transmitter antennas are located at different heights (1.5, 5, and 7 m) in order to investigate both V2V and V2I scenarios. A truck was used to obstruct the LOS between transmitter and receiver, and a large number of geometrical combinations of the scenario were explored. The statistical analysis of the measurement shows how in the V2V case, the experienced shadow levels are approximately 5 dB higher than in the V2I scenarios, where the shadow levels depend on the transmitter antenna height, reaching maximum values of 21-23 dB. The statistical analysis also shows that the differences in shadow level due to the non-symmetries of the obstacle truck are in the order of approximately 2 dB. A simple 3D ray-tracing simulation is validated against the measurements, showing a good match with a RMSE of 4.1 dB. Based on both measurements and ray-tracing data, a simple deterministic shadowing model, useful for implementation in system level simulators, is presented, as a first step towards a more dynamic and scalable shadowing model.**

I. Introduction

Autonomous vehicles and safety-improving driving applications, such as warnings of hazardous road conditions and overtaking vehicles, expected in the near future, are to be enabled by vehicular communications. These new use cases impose strict requirements to the communication link in terms of reliability of 99.999 % and latency below 5 ms [1]. The vehicular communication will rely on both vehicle-to-vehicle (V2V) and vehicle-to-infrastructure (V2I) communication, combined termed as V2X. Due to the reliability and latency requirements of the V2X communication and the criticality of the use cases, even the shortest obstruction of the communication link is an issue. Therefore, the characteristics of the communication channel and, especially, the shadow loss due to large vehicles, are of renewed interest for many researchers.

Until recently, dedicated short range communication radio access technologies (RATs) such as 802.11p have been the key focus area for vehicular communication. These technologies mainly rely on V2V communication and, therefore, channel models where both transmitter and receiver are mobile and have similar heights, have been studied extensively. In previous works, large scale propagation is modeled by single and dual slope log-distance path loss models, geometry-based models or ray-tracing techniques [2]. Specifically addressing the shadow fading caused by large vehicles, previous studies, based on both real measurements and ray tracing predictions [3,4], reported an additional loss of 12-20 dB depending on the distance between transmitter, receiver, and the vehicle obstructing the line-of-sight (LOS).

Nowadays, the V2I scenario is under discussion. As opposed to V2V case, this scenario may benefit from a higher transmitter position and thus be less prone to large vehicle shadowing. Unfortunately, this temporary shadowing condition has not been as extensively investigated as in the V2V case [2]. Due to the stringent reliability and latency requirements, critical to vehicular communications, an accurate characterization of the shadowing phenomena is still needed in the unexplored V2I scenarios, in order to determine whether, for example, autonomous vehicles can be supported by the infrastructure. In this direction, existing ray-tracing studies have examined road side unit (RSU) scenarios with blind corners [5] without providing specific results for large vehicle shadow loss. Measurements have also been conducted in real RSU scenarios, however the focus was done on small scale fading models [6], and packet delivery rate evaluations [7]. These evaluations show that non-line-of-sight (NLOS) conditions caused by large vehicles, buildings and vegetation, are the most critical issue for vehicular communication, thus underlining the necessity of understanding V2I large vehicle shadowing. This is also evident from the recent V2X surveys [2,8,9], which identify large vehicle shadowing as a key area for future research.

In this context, this paper complements the previous work by presenting a measurement-based evaluation of large vehicle shadowing in a controlled scenario. An extensive measurement campaign was performed for different combinations of transmitter positions and heights (1.5, 5 and 7 m), with a receiver located at 1.5 m, emulating both V2V and V2I links in a 4-lane road scenario at 5.8 GHz. This particular frequency band is the selected band for road safety and traffic efficiency

TABLE I: Summary of the V2X TX/RX configurations and TX positions considered during the measurement campaign.

					TX re-deployment positions [x,y] - shown on Figure 1					
TX	f_c [MHz]	Link type	h_{TX} [m]	h_{RX} [m]	1	2	3	4	5	6
Mast_1	5800	V2I	7	1.5	[-2,0]	[-2,-6]	[-2,-40]	[-5,-40]	[-5,-6]	[-10,0]
Mast_2	5801	V2I	5	1.5	[-2,0]	[-2,-6]	[-2,-40]	[-5,-40]	[-5,-6]	[-10,0]
Mast_3	5802.2	V2V	1.5	1.5	[-2,0]	[-2,-6]	[-2,-40]	[-5,-40]	[-5,-6]	[-10,0]
Van_1	5803.6	V2I	7	1.5	[-2,+40]	[-2,+6]	[-5,+6]	[-5,0]	[-5,+40]	[-5,+40]
Van_2	5805.2	V2I	5	1.5	[-2,+40]	[-2,+6]	[-5,+6]	[-5,0]	[-5,+40]	[-5,+40]
Trolley_1	5807	V2V	1.5	1.5	[-2,+6]	[-2,+40]	[-5,+40]	[-5,+6]	[-5,0]	[-5,0]

applications [10]. A truck was placed in different positions obstructing the LOS between transmitters and receiver, creating many different shadowing situations. A statistical analysis is performed over the measurement data in order to quantify and compare the different shadow levels and dynamics expected in the diverse V2V and V2I scenarios. The measurements are compared to ray-tracing simulations, providing valuable input for accurate modeling of V2X communication scenarios. Based on both the measurements and the ray-tracing simulations, an initial version of a deterministic shadowing model, useful to be used in system level simulations, is presented. The future research directions towards a complete realistic dynamic shadowing model are presented in the paper as well.

The rest of the paper is structured as follows: Section II describes the different aspects related to the measurement campaign. Section III presents the statistical analysis of the measurement results and the discussion based on the different V2X scenarios. Section IV introduces the ray-tracing simulations and the comparison with the measurements. Section V presents the road-map towards a complete realistic and dynamic shadowing model, including an initial version of a deterministic large vehicle shadowing model. Finally, Section VI concludes the paper.

II. Measurement Campaign

A. Measurement Scenario

The measurement campaign was performed in a driving school located a few kilometers north from Aalborg, Denmark. A dedicated V2X propagation scenario was reproduced over a rectangular flat pavemented area of approximately 45x95 m. The layout of the considered scenario is an 80 m long section of a 4-lane road, resembling the typical wide-street vehicular case in any mid-sized European city, with 2 lanes per driving direction. Each of the lanes was marked by using traffic cones, considering a lane width of 3.5 m (which is the European average width for all types of pathways: urban, rural and highways [11]). A set of 6 transmitter (TX) antennas was deployed at different heights (h) on a mast (7, 5 and 1.5 m), a van (7 and 5 m) and a trolley (1.5 m), emulating different RSUs, and re-deployed several times by swapping them across the 11 different positions illustrated in Figure 1. A single receiver (RX) antenna was mounted on a trolley at average vehicular height (1.5 m) [12], emulating a car roof antenna. By considering this setup, various V2X combinations are explored. This includes both the V2I and V2V cases, as detailed in Table I.

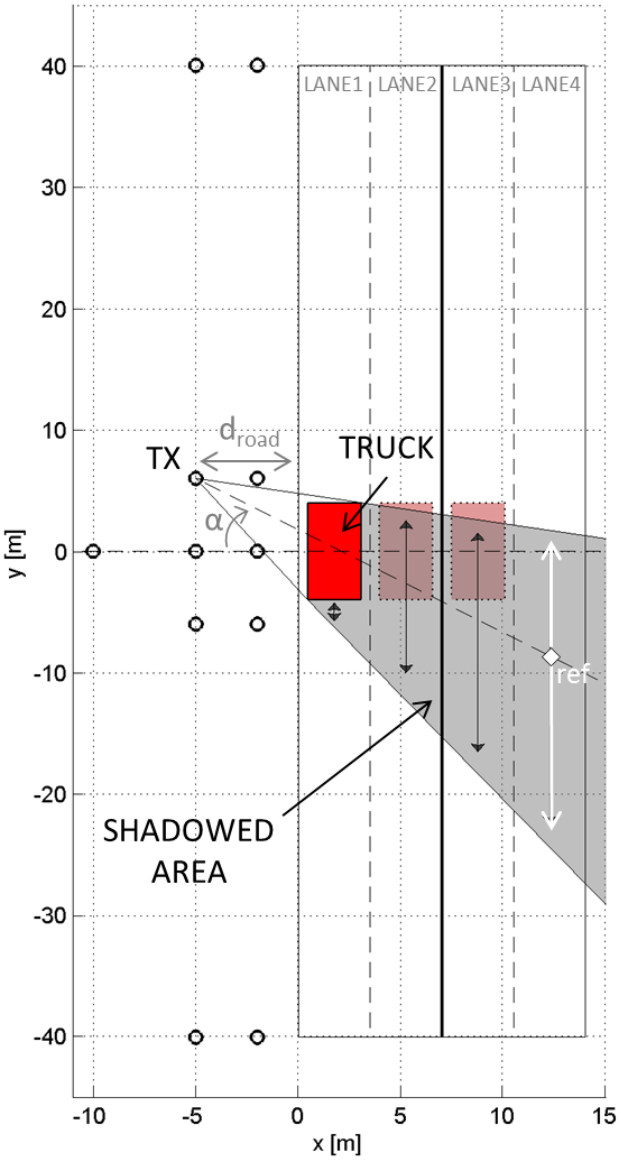

Fig. 1: Overview description of the measurement scenario.

The V2X link measurements were performed by driving the RX trolley at walking speed (5 km/h in average) along each of the 4 lanes, recording simultaneously the signal strength from the 6 different transmitters, each of which was transmitting an independent narrow-band continuous wave (CW) signal. The selected orthogonal frequencies of operation (f_c) are detailed in Table I.

Fig. 2: Obstacle truck (in the foreground), and mast/van containing part of the transmitters (in the background).

The different V2X links were obstructed by placing the large vehicle (truck), shown in Figure 2, in the central part of the road section as depicted in Figure 1. The dimensions of the truck were approximately 8x2.6x3.6 m (length x width x height). Diverse shadowing conditions were created over the different lanes, depending on the geometry of the scenario: dimensions of the obstacle, position of the obstacle (e.g. lane number over which the truck is placed), height of the TX, distance of the TX to the first lane (d_{road}), height of the RX, position of the RX (e.g. lane number over which the RX is located), and interaction angle (α) between TX and obstacle (defined as the angle relative to the direction of normal incidence on the left side of the truck).

In order to make the study more statistically significant, a large number of different scenario situations were created. Each of the aforementioned re-deployments across the 11 different TX positions was independently performed for the obstacle truck located on lanes 1, 2, and 3. All in all, by considering the 3 different truck positions, 3 antenna height combinations, 11 TX positions, and 4 lanes covered by the RX, the measurement examined a total of 176 different geometrical combinations.

B. Setup, Calibration & Data Processing

At the TX side, NI USRP-2953R devices were used to generate each of the CW signals with a constant output RF power (P_{TX}) of 10 dBm. These signals were fed into the correspondent TX antenna by using coaxial cables of different lengths depending on the TX antenna height. All the TX antennas were standard dipoles with a gain (G_{TX}) of approximately 3.5 dBi. Only vertical polarization was explored.

At the RX side, an omnidirectional antenna H+S SWA 0859/360/4/10/V of approximately 6 dBi of gain (G_{RX}) was used. A jumper cable was used to transfer the received signals into the receiver. A R&S TSWM universal radio network analyzer was used as RX, recording the signal strength of all the different CWs simultaneously at a sampling rate of 10 Hz. An average of approximately 576 received power (P_{RX}) samples were recorded per driven lane. In order to remove fast-fading effects, the received power samples were averaged over chunks of 1 m distance (20 wavelengths), resulting in 80 samples per lane.

The combined cable loss (L_c) was measured and calibrated, resulting in 3.7 dB for the links with TX antenna at 1.5 m, 8.4 dB for the links with TX antenna at 5 m, and 9.5 dB for the links with TX antenna at 7 m. The sensitivity of the scanner used in the measurement was -115 dBm, which combined with the previous values according to (1) leads to maximum measurable path loss (PL_{meas}) of 138-144 dB.

$$PL_{meas} = P_{TX} - P_{RX,meas} + G_{TX} + G_{RX} - L_c \quad \text{[dB]} \quad (1)$$

To characterize the shadowing effect, excess path loss (ΔPL) is defined in (2) as the difference between the measured path loss and free space path loss ($FSPL$). In the scenario explored, with only the obstacle truck obstructing the line-of-sight (LOS) between TX and RX, a negative excess path loss ($\Delta PL < 0$) would indicate favorable contributions to the received signal, most likely due to reflections on the truck. While, on the other hand, positive excess path loss ($\Delta PL > 0$) would indicate negative contributions to the propagation, mainly due to the obstruction by the truck and suggesting that the RX is in a shadowed area. The latest is the main focus of this paper.

$$\Delta PL = PL_{meas} - FSPL \quad \text{[dB]} \quad (2)$$

In order to further calibrate the system and the calculations, a LOS measurement (without the obstacle truck) was performed along all the 4 lanes (+3 extra, in order to enlarge the calibration range) with the transmitters in re-deployment configuration 6. In the end, the calibration measurement covered distances between 5 and 120 m, including a large number of both elevation and azimuth angles. From the result, it was possible to verify that the calibrated LOS path loss obtained matched quite well the theoretical FSPL with an average root mean square error (RMSE) of 4.4 dB, considering data from all the different TX antenna heights. This result validates the use of the FSPL as a correct reference for the excess path loss calculation, over the entire measurement area defined.

III. Measurement Results

All the measurement cases were independently post-processed using (1) and (2) to obtain the excess path loss in the different situations. A statistical analysis was performed on the entire set of resulting empirical data.

First, the overall excess path loss per scenario was explored. Figure 3 presents the cumulative distribution functions (CDF) of the measured excess path loss for the different V2I scenarios with TX antennas at 5 and 7 m, V2V scenarios with TX antenna at 1.5 m, and the combined V2X scenario that includes all the measurement data from all the different TX antenna heights. These empirical distributions are taken to model the probability of large vehicle shadowing being above or below a certain threshold. As it can be seen, the probability of being above any particular threshold value is higher for lower TX antenna heights. This means that, in case of being shadowed by a large vehicle, the impact is more significant for the V2V scenario than for the V2I scenario. For example, in the V2V scenario, the probability of experiencing a shadow level higher

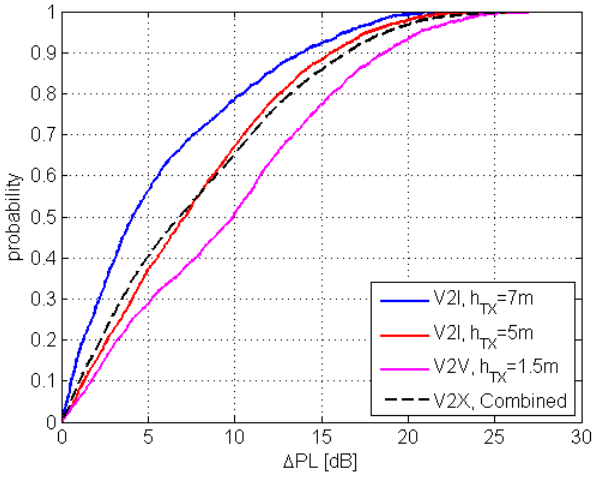

Fig. 3: Shadow level probabilities for the different V2V, V2I and combined V2X scenarios.

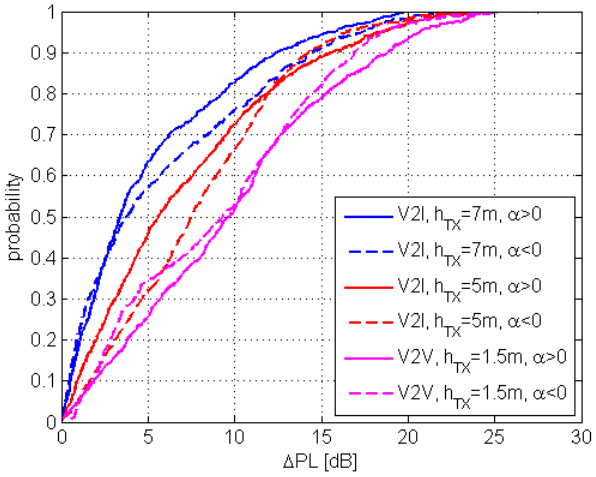

Fig. 4: Shadow level probabilities for the different V2V and V2I scenarios classified per interaction angle.

than 10 dB is 50%, while in the V2I scenario this probability is reduced to 35% and 20% for TX at 5 and 7 m, respectively. The maximum shadowing values experienced in the measurement were 21-23 dB for the V2I scenario and 27 dB for the V2V scenario. In the case of considering the entire V2X scenario as a whole, without distinguishing between different TX antenna heights or type of links (V2V/V2I), it can be seen, how the resulting shadow level probability is very similar to the one for the intermediate TX antenna height.

The extensive measurement campaign, performed with transmitters in different positions, allowed to analyze other geometrical characteristics of the shadowing. Figure 4 presents the same distributions as before, but separated for positive and negative interaction angles (α). These results allow to understand what is the impact of the non-symmetrical structure of the obstacle truck. As it can be seen, for the V2I scenario at both TX antenna heights, higher shadow levels are in general experienced for negative interaction angles ($\alpha < 0$). This is due to the fact that, for these angles, the container is the closest part of the truck to the TX, which is approximately 0.5 m taller than the cabin and, therefore, causes larger shadowing. In average, the differences in shadow level due to the non-symmetry of the obstacle truck are found to be in the order of approximately 2 dB. In the case of the V2V scenario, the non-symmetry impact is even smaller.

IV. Comparison with Ray-tracing

In order to gain further insight on the different possibilities for large vehicle shadowing characterization, the measurement campaign was reproduced in a commercial ray-tracing tool [13]. Figure 5 shows the simple 3D model of the measurement scenario composed of a flat surface of dimensions 100x60 m and a simplified block model of the obstacle truck. Both the ground surface and the truck were modeled with standard materials available in the tool database: medium dry floor and metal, respectively. The simulations for computation of path loss were performed with 3D standard ray-tracing, with a resolution of 0.25 m and basic simulation settings: LOS path

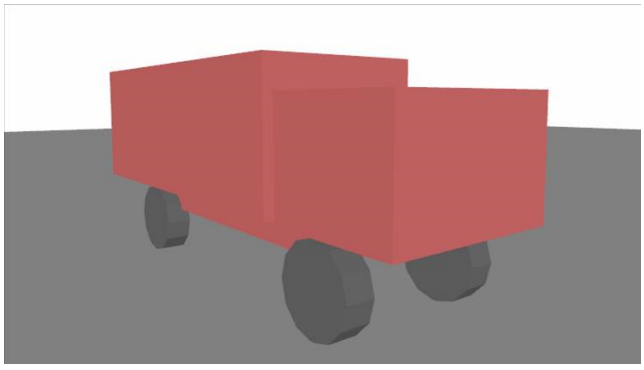

Fig. 5: Simple 3D ray-tracing model of the obstacle truck.

loss exponent of 2, reflection and diffraction losses based on default permittivity and conductivity values of the different materials, and maximum 2 ray interactions.

Figures 6 and 7 show two examples of measurements (M) compared to ray-tracing (RT) predictions. They are similarly arranged in 4 sub-figures. Sub-figure a) displays the averaged excess path loss with a resolution of 1 m (80 samples per lane), computed from the measurements by following the procedures previously mentioned in Section II. Sub-figure b) contains the processed ray-tracing results, and it is directly comparable with Sub-figure a). In this case, the averaged excess path loss per lane has been computed by translating the original ray-tracing predictions with a resolution of 0.25 m, displayed in Sub-figure c), to the lane resolution of 1 m by applying exactly the same averaging procedures as to the measurements. In practice, the processed results are more representative of the shadow levels that a car would experience in the real world, due to potential RX antenna pattern irregularities and the different ray contributions to the received signal. Finally, Sub-figure d) presents an individualized comparison of the measurement and ray-tracing data per different lane, including RMSE values and cross-correlation coefficients (xcorr), giving a numerical indication on how good is the match between measurements and simulations.

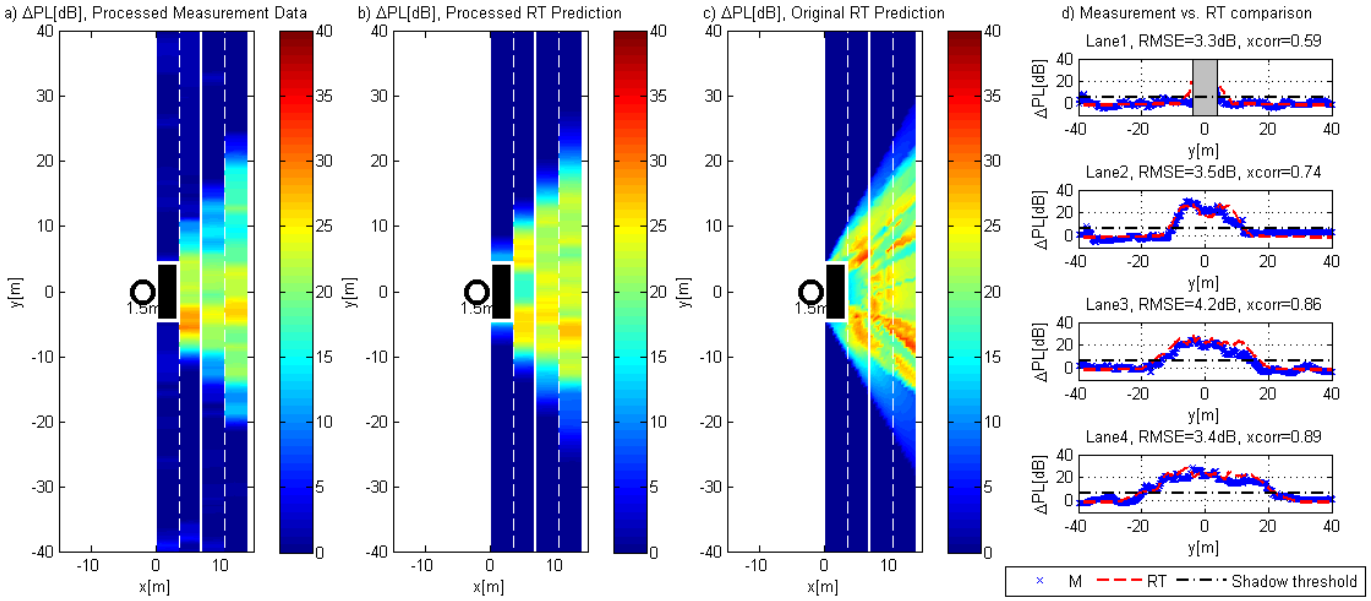

Fig. 6: Comparison of measurements with ray-tracing for one of the V2V cases explored ($h_{TX} = 1.5$ m, $h_{RX} = 1.5$ m, $d_{road} = 2$ m, $\alpha = 0°$, obstacle truck on lane 1).

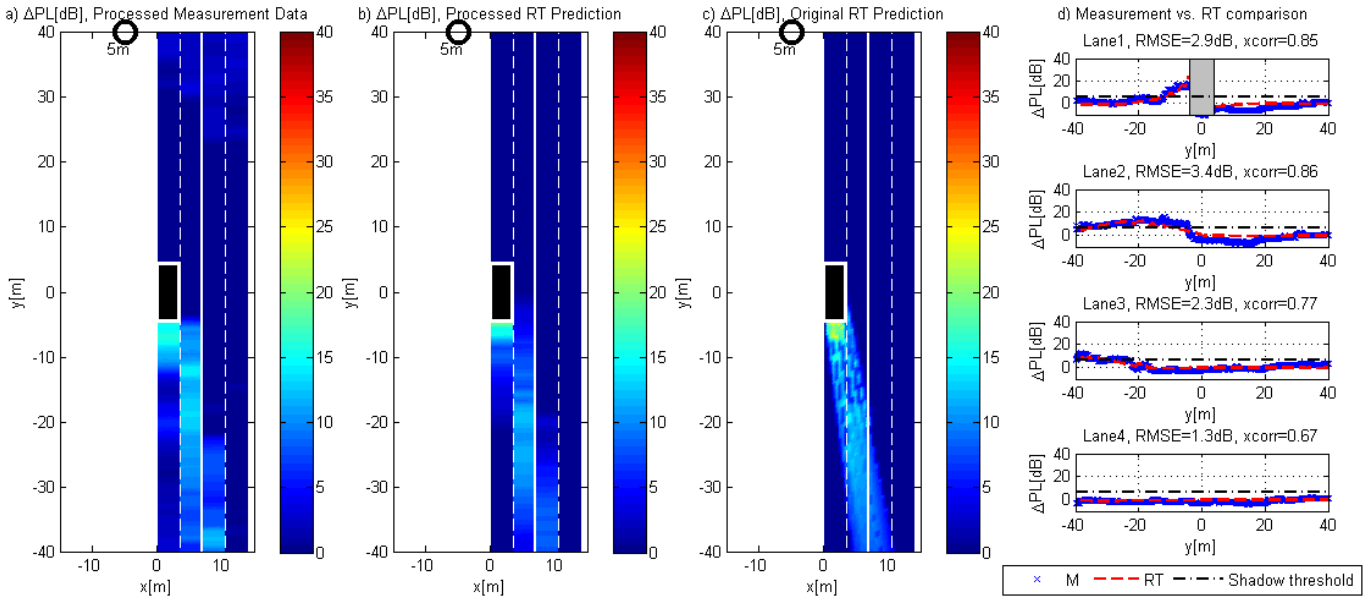

Fig. 7: Comparison of measurements with ray-tracing for one of the V2I cases explored ($h_{TX} = 5$ m, $h_{RX} = 1.5$ m, $d_{road} = 5$ m, $\alpha = 80°$, obstacle truck on lane 1).

With focus on the results now, in Figure 6, one of the V2V cases with the obstacle truck placed on lane 1 is presented. The 1.5 m height TX antenna was located at position [-2,0], with an interaction angle of zero, which means that the incident angle is perpendicular to the left side of the truck. As it can be seen from all sub-figures a), b) and d), the ray-tracing predictions show a good match to the measurements. For this particular case, an average RMSE of 3.6 dB and xcorr coefficient of 0.77 were obtained. This was the explored case with the strongest shadowing conditions, and some details can be observed. One of them is that, by looking at the data from lane 2 in sub-figure d), it can be seen how both the measurement and ray-tracing excess path loss present a small valley (reduction of approximately 6 dB) at the central position. This is due to the positive contribution of reflections of the signal on the ground below the truck between wheel axes. This also appreciable in the heatmaps. The second detail that is worth to be mentioned is that, especially in the measurement data from lanes 2 and 3, it is noticeable that, in shadowed areas, the excess path loss is slightly smaller for lane positions with positive ordinate ($y > 0$). This is due to the aforementioned fact that the obstacle truck was not symmetric, and the cabin shadows a few dB less than the container. Under this particular V2V configuration, cars driving on shadowed areas of the lanes would experience maximum shadow levels of approximately 22-27 dB.

The second case, in Figure 7, presents a V2I example. The TX antenna was located at 5 m in position [-5,+40]. The obstacle truck was still placed on lane 1, as in the previous V2V example. In this case, the average RMSE was 2.5 dB, with a xcoor coefficient of 0.79. While in the previous case shadowing on the first lane was negligible, meaning that a car will experience no shadow impact by driving close in-front/behind the truck in the same lane. In this case, due to the larger interaction angle, some shadowing is created over the lane on which the obstacle truck is positioned (lane 1). The results illustrate the benefit of having elevated TX antenna positions in the V2I scenario. Even though larger areas are shadowed, the shadow levels, measured in excess path loss, are smaller than in the previous V2V scenario. In this case, the maximum shadow levels experienced per lane were in the range 0-18 dB.

It is nontrivial to present individually all the different cases considered in the study, but the conclusion is that with very simple ray-tracing simulations, with not very detailed 3D models or material characterization, it is still possible to achieve a quite accurate level of prediction of both geometry and shadow levels. Considering all the different combinations explored, the overall RMSE was 4.1 dB, while the average xcorr coefficient was 0.65.

V. Dynamic & Scalable Shadowing Model

The results and observations presented in this paper are part of the initial study towards the development and calibration of a dynamic and scalable shadowing model for system level simulation of V2X communications. As a first step, it is possible to propose a stochastic model based on the empirical distribution in Figure 3, or the corresponding sample-based distribution from ray-tracing simulations. The approach, illustrated in Figure 8, can be useful for simple static snap-shot based system level simulations where one wants to ignore the geometric detail, and instead apply the shadowing state by probabilistic means. It is envisaged here that the state of being shadowed can be determined probabilistically based on the traffic density, since denser traffic implies a higher probability of being shadowed. If shadowed, the actual fading state (ΔPL) can be determined from the distributions in Figure 3 using the inverse percentile transformation method, and added to the overall link path loss (PL).

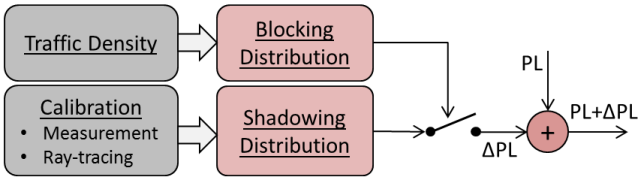

Fig. 8: Overview of the intended future dynamic and scalable shadowing model for V2X communications.

A more deterministic model, based on the actual geometry of the link and the obstructing vehicle, can be computed from more detailed information extracted from the measurements.

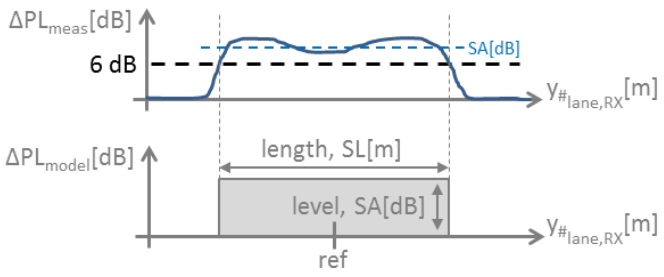

Fig. 9: Initial deterministic shadow model: calculation of the SA and SL coefficients and application example.

For instance, based on the different combinations of V2V and V2I TX antenna height (h_{TX}), distance from the TX to the first lane of the road (d_{road}), interaction angle between the TX and the truck (α), target lane ($\#_{lane,RX}$), and lane where the obstacle truck is located ($\#_{lane,truck}$), the model output can be summarized in terms of the shadowing path loss (fading state) over a particular lane, and the spatial length over which this occurs (fading state duration). Such a model can be tailored for time-dynamic system level simulations.

The model output, defined in (3), is given as a look-up table in Table II in terms of shadow amplitude (SA, in dB) and shadow length (SL, in m), relative to the central position (ref) defined by the intersection between the target lane and the interaction angle (α) - see lane 4 on Figure 1 for visual reference. The pairs of values have been determined by applying a 6 dB reference threshold on the data, from either measurements (M) or ray-tracing (RT) simulations, so that a bounded region results for the shadowing length. Each corresponding pair (SA,SL) is defined over the length of the lane where measured or simulated data exceeds this threshold, as depicted in Figure 9.

$$(SA, SL) = f\left(h_{TX}, d_{road}, \alpha, \#_{lane,RX}, \#_{lane,truck}\right) \quad (3)$$

As an example on how the SA and SL coefficients have been calculated, the 6 dB shadow threshold has been plotted as a reference in Figures 6.d and 7.d, and the corresponding output values have been highlighted in Table II. The reference value for the threshold was selected due to the fact that, for the explored scenario, diffraction on the truck wedges is the main propagation mechanism into the shadowed areas, and 6 dB is the minimum knife-edge diffraction loss when half of the TX antenna beam is blocked by the truck [14]. A sensitivity analysis was performed on the selected reference threshold value, finding very similar values for 0 dB and 3 dB thresholds, with small average SA differences of 0.2 dB and slightly larger (1.2-2.5 m) SL values.

It should be noticed that the interaction angles in Table II have been classified as 0, $\pm$60 and $\pm$90 degrees. Each of them encompass the different TX positions with ordinate (y) 0, $\pm$6 and $\pm$40 m, respectively. This has been done for simplification of the model, to make a clearer distinction in interaction angle (normal incidence, intermediate condition, and grazing angle). This initial look-up approach of the model has some limitations, due to the size of the scenario explored. In this

TABLE II: Model look-up table with the different measured (M) and simulated (RT) shadow lengths (SL) in m and shadow amplitudes (SA) in dB at 5800 MHz.

				Obstacle truck on lane 1				Obstacle truck on lane 2			Obstacle truck on lane 3	
d_{road}	α	h_{TX}		Lane 1	Lane 2	Lane 3	Lane 4	Lane 2	Lane 3	Lane 4	Lane 3	Lane 4
[m]	[^{o}]	[m]		[m] / [dB]	[m] / [dB]	[m] / [dB]	[m] / [dB]	[m] / [dB]	[m] / [dB]	[m] / [dB]	[m] / [dB]	[m] / [dB]
2	90	7	M	14 / 11.3	4 / 7.1	0 / 0	0 / 0	9 / 15.4	13 / 8.3	0 / 0	6 / 12	14 / 9.9
			RT	12 / 11.5	0 / 0	0 / 0	0 / 0	7 / 12.6	15 / 9.1	0 / 0	5 / 12.8	14 / 9.3
		5	M	14 / 10.4	27 / 9.4	2 / 27.5	0 / 0	9 / 13.5	22 / 10.1	5 / 6.7	4 / 11.8	19 / 10.6
			RT	12 / 10	22 / 8.8	0 / 0	0 / 0	7 / 12.1	25 / 9.3	12 / 7.3	4 / 15	20 / 8.6
		1.5	M	3 / 10.9	4 / 9.8	0 / 0	0 / 0	11 / 12.7	13 / 10.4	6 / 8.9	0 / 0	16 / 12.3
			RT	11 / 12.1	1 / 6.2	0 / 0	0 / 0	9 / 11	11 / 8.2	3 / 6.5	5 / 12.6	12 / 8.9
	60	7	M	3 / 11.9	9 / 12.3	4 / 7.2	0 / 0	4 / 11.6	10 / 12.6	10 / 8.8	4 / 11.9	6 / 11.7
			RT	2 / 10.5	9 / 9.6	0 / 0	0 / 0	1 / 8.5	10 / 16.6	0 / 0	1 / 6.3	10 / 14.8
		5	M	6 / 15.3	15 / 16	14 / 11.6	2 / 6.2	4 / 18.2	11 / 17.4	13 / 14.8	6 / 12.5	11 / 15.2
			RT	4 / 13.3	14 / 19.6	0 / 0	0 / 0	2 / 7.8	13 / 19.4	13 / 11.6	1 / 8	12 / 17.4
		1.5	M	15 / 10.1	22 / 16.5	42 / 18.1	40 / 14.6	3 / 17.5	11 / 18.3	18 / 14	5 / 12.5	11 / 16.9
			RT	5 / 12.9	25 / 17.8	36 / 13.6	40 / 16.4	2 / 11.8	16 / 19	20 / 12.9	1 / 10.1	14 / 16.5
	0	7	M	7 / 11.2	7 / 12.7	3 / 7.3	3 / 8.3	1 / 6.1	13 / 11	8 / 8.7	0 / 0	12 / 13
			RT	2 / 9.1	9 / 9.4	0 / 0	0 / 0	0 / 0	11 / 15.3	0 / 0	0 / 0	11 / 13
		5	M	6 / 14.3	22 / 12.1	8 / 11.7	2 / 8	0 / 0	16 / 13.3	15 / 13	1 / 7.5	9 / 15.4
			RT	3 / 8.3	15 / 16.6	0 / 0	0 / 0	0 / 0	14 / 15.6	12 / 11.9	0 / 0	12 / 15.1
		1.5	M	**2 / 8.2**	**23 / 14.6**	**31 / 15.8**	**42 / 17.7**	0 / 0	13 / 17.6	16 / 14.7	0 / 0	10 / 15.3
			RT	**4 / 10.6**	**24 / 20**	**33 / 19.7**	**43 / 19**	1 / 15.5	15 / 24.6	20 / 16	1 / 9.6	12 / 20.3
	-60	7	M	4 / 12.1	5 / 7	0 / 0	3 / 9.9	4 / 17.9	10 / 12.4	0 / 0	5 / 15.4	11 / 15.2
			RT	4 / 11.4	8 / 8.6	0 / 0	0 / 0	2 / 10.3	12 / 13.7	0 / 0	1 / 12	12 / 12.2
		5	M	2 / 12.7	15 / 9.9	0 / 0	0 / 0	5 / 16.3	12 / 14.4	13 / 9.9	4 / 17.5	11 / 15.3
			RT	6 / 10.4	18 / 13.5	0 / 0	0 / 0	2 / 11.9	15 / 15.5	14 / 10.5	1 / 14.4	14 / 14.9
		1.5	M	5 / 15.4	26 / 16.1	26 / 11.3	41 / 16	1 / 12.1	11 / 14.1	14 / 12.4	0 / 0	9 / 15.2
			RT	6 / 14.9	23 / 18.2	35 / 14	41 / 17.1	2 / 18.9	15 / 19.5	20 / 13.3	1 / 18.4	13 / 17
	-90	7	M	15 / 11.4	0 / 0	0 / 0	0 / 0	8 / 12.3	15 / 9.7	0 / 0	2 / 13.6	11 / 11.8
			RT	16 / 10.7	0 / 0	0 / 0	0 / 0	9 / 11.3	19 / 8.8	0 / 0	6 / 11.7	18 / 8.7
		5	M	36 / 9.2	30 / 11.6	1 / 7.2	0 / 0	13 / 9.9	31 / 10	19 / 7.8	2 / 12.7	17 / 10.1
			RT	16 / 9.5	23 / 8.8	0 / 0	0 / 0	7 / 12.1	27 / 9.4	8 / 7.1	5 / 12.9	21 / 8.7
		1.5	M	19 / 11.3	25 / 8.8	3 / 7.1	0 / 0	4 / 16.1	19 / 10.4	16 / 9.3	5 / 13.1	19 / 11
			RT	12 / 13.8	1 / 6.1	0 / 0	0 / 0	9 / 13.5	11 / 8.2	6 / 6.7	5 / 16.2	15 / 8.3
5	90	7	M	7 / 13.2	10 / 8.2	0 / 0	0 / 0	5 / 11.4	13 / 9.7	0 / 0	4 / 9.1	13 / 11.2
			RT	8 / 12	16 / 8.5	0 / 0	0 / 0	5 / 13	18 / 10.1	0 / 0	4 / 11.9	16 / 9.9
		5	M	**9 / 11.4**	**20 / 9.9**	**15 / 7.4**	**0 / 0**	5 / 11	18 / 9.8	21 / 8.6	2 / 9.6	16 / 10.1
			RT	**8 / 11.4**	**26 / 9.2**	**14 / 8**	**0 / 0**	5 / 13.3	23 / 9	18 / 8.8	3 / 14.2	17 / 9.3
		1.5	M	13 / 8.5	18 / 10.3	12 / 9.6	0 / 0	4 / 9.8	18 / 10.4	25 / 9.5	2 / 9.2	16 / 11.4
			RT	10 / 10.7	11 / 7.7	4 / 6.3	0 / 0	5 / 12.7	15 / 10.9	7 / 6.4	3 / 13.9	14 / 10.4
	60	7	M	4 / 14.7	8 / 14.9	0 / 0	0 / 0	0 / 0	15 / 12.8	7 / 11.3	0 / 0	11 / 14.5
			RT	1 / 9.6	10 / 16.1	0 / 0	0 / 0	1 / 6.4	10 / 17.1	0 / 0	0 / 0	10 / 15.6
		5	M	5 / 17.1	12 / 17.4	11 / 13.1	12 / 8.1	1 / 7.3	13 / 14.4	12 / 14.5	0 / 0	10 / 15.9
			RT	2 / 8.3	13 / 20	13 / 12.3	0 / 0	1 / 8.2	12 / 16.9	13 / 14.3	0 / 0	12 / 17.5
		1.5	M	4 / 18.3	15 / 17.4	19 / 14.7	26 / 14	0 / 0	12 / 17.2	14 / 14.3	0 / 0	10 / 15
			RT	2 / 12.8	17 / 19	21 / 13.7	26 / 11.2	1 / 10.7	13 / 19.4	16 / 11.9	0 / 0	12 / 17.4
	0	7	M	6 / 12	10 / 13.1	9 / 8.1	0 / 0	2 / 8.1	13 / 12.6	7 / 6.6	1 / 10.1	9 / 13
			RT	1 / 6.3	11 / 14.9	0 / 0	0 / 0	0 / 0	11 / 14.9	0 / 0	0 / 0	11 / 13.1
		5	M	6 / 14.4	16 / 13.7	20 / 11.3	13 / 9	3 / 8.1	12 / 14.6	14 / 12.5	1 / 6.6	10 / 13.8
			RT	1 / 6.3	14 / 16.1	12 / 12.9	0 / 0	0 / 0	12 / 15	14 / 13	0 / 0	12 / 14.3
		1.5	M	7 / 17.2	12 / 16	18 / 15.3	21 / 12.6	2 / 7.4	10 / 17.5	13 / 15.2	2 / 7	10 / 16.2
			RT	2 / 11.2	15 / 25.7	20 / 17.6	25 / 13.7	1 / 10.2	12 / 23.1	16 / 13.2	1 / 6.4	12 / 17.2
	-60	7	M	4 / 15.6	8 / 13.7	2 / 6.7	0 / 0	4 / 16.5	11 / 13.8	5 / 7.6	0 / 0	9 / 12.8
			RT	2 / 10.6	12 / 13.2	0 / 0	0 / 0	1 / 12.3	12 / 14	0 / 0	1 / 12.3	12 / 12.7
		5	M	4 / 17.4	13 / 14.4	13 / 11.6	7 / 6.7	4 / 17.9	13 / 14.5	14 / 12.8	0 / 0	8 / 16.4
			RT	2 / 12.1	16 / 15.1	14 / 11.3	0 / 0	1 / 14.3	13 / 15.6	13 / 12.9	1 / 15.2	12 / 16.6
		1.5	M	4 / 14.8	12 / 14.7	14 / 12.7	18 / 12.9	0 / 0	10 / 16.5	13 / 12.2	0 / 0	8 / 16.6
			RT	3 / 15.5	16 / 19.5	20 / 14.5	25 / 11.8	1 / 19.4	13 / 19.2	15 / 12.5	1 / 14.8	12 / 17
	-90	7	M	11 / 13	14 / 10.3	0 / 0	0 / 0	6 / 18.2	16 / 11.9	3 / 7	6 / 16.4	13 / 11.4
			RT	10 / 11.1	20 / 8.3	0 / 0	0 / 0	6 / 11.8	19 / 10.5	0 / 0	5 / 11.9	17 / 9.7
		5	M	17 / 11.9	34 / 11	16 / 9.2	0 / 0	6 / 14.5	22 / 10.9	23 / 9.9	5 / 15.8	17 / 11.5
			RT	7 / 12.2	29 / 9.3	11 / 7.8	0 / 0	5 / 13	21 / 9.4	22 / 8.4	5 / 11.8	15 / 9.1
		1.5	M	8 / 11.1	23 / 10.5	20 / 8.8	0 / 0	0 / 0	0 / 0	0 / 0	4 / 11	13 / 12
			RT	10 / 13	12 / 7.5	5 / 6.9	0 / 0	5 / 16.6	14 / 11.1	8 / 6.6	5 / 14.5	14 / 10.3
10	0	7	M	5 / 12.2	10 / 12.3	9 / 10	2 / 8.5	1 / 7	11 / 12.2	10 / 10.8	0 / 0	10 / 13
			RT	0 / 0	11 / 14	9 / 8.3	0 / 0	0 / 0	10 / 14.1	9 / 10	0 / 0	10 / 15.1
		5	M	6 / 11.6	11 / 14	12 / 12.5	15 / 11.1	0 / 0	12 / 12.4	11 / 12.4	0 / 0	9 / 13.5
			RT	0 / 0	12 / 14	14 / 13.2	12 / 10.8	0 / 0	11 / 16.3	12 / 13.4	0 / 0	11 / 16.6
		1.5	M	4 / 16.4	11 / 15.4	12 / 12.2	13 / 11.5	0 / 0	12 / 13.7	11 / 11.9	0 / 0	8 / 13.7
			RT	1 / 8.6	12 / 20.2	14 / 12.7	14 / 10.3	0 / 0	11 / 19.7	10 / 12.6	0 / 0	10 / 18.8

respect, shadow lengths may be larger in reality than what is given in the table, for TX positions at large interaction angles. However, a minor error is expected in shadow amplitude. This can be easily understood from, for example, the V2I example presented in Figure 7, where the shadow would be further extended on lanes 2-3 for positions with ordinate smaller than -40 m. The average difference between the coefficients calculated over the measurement data or the ray-tracing data is approximately 0.4 dB in shadow amplitude, and smaller than 1 m in shadow length.

With this initial version of the model, it is possible to simulate only very basic V2X scenarios and situations (e.g. a car overtaking a truck). However, for that particular situation, it would be already possible to perform a sensitivity analysis of different V2I deployment configurations considering, for example, different RSU inter-site distances and antenna heights, for various car speeds. This will provide some initial insights on how the shadowing due to large obstacles may affect the reliability of the link, even though it is only for a short period of time. The future model will, of course, consider more complex situations, including more dynamic aspects of the scenario.

VI. Conclusions

This paper presented a measurement-based evaluation of the impact of large vehicle shadowing on V2X scenarios at 5.8 GHz. An extensive measurement campaign was performed by considering several V2V and V2I configurations in a practical 4-lane road section scenario. The RX antenna height was fixed to average vehicular height (1.5 m), and the TX antenna heights were fixed to 5 and 7 m for the V2I scenarios, and 1.5 m for the V2V cases. Different shadow conditions were created by placing a large truck at different positions, obstructing the LOS between TX and RX.

The analysis of the measurement data shows how, in case of being shadowed by a large vehicle, the impact is more significant in the V2V scenario than in the V2I scenario, which benefits from the elevated TX antenna position. The maximum shadowing levels experienced were 27 dB in the V2V scenario, 23 dB in the V2I scenario with TX antenna height at 5 m, and 21 dB in the V2I scenario with TX antenna height 7 m. The empirical distributions are given in the paper, and are useful for statistical characterization of the V2X scenario. The impact to the shadow level due to non-symmetries of the obstacle truck was also evaluated, finding small average variations of approximately 2 dB.

The measurements were compared to 3D ray-tracing simulations, showing a good match with a RMSE of 4.1 dB. From these results it can be concluded that ray-tracing simulations, based on 3D models with limited details and material characterization, can still result in accurate levels of predictions of both geometry and shadow levels.

The future work was also introduced in the paper, presenting the roadmap towards a dynamic and scalable shadowing model suitable for simulation of V2X communication systems. As an alternative initial approach, a look-up table-based deterministic shadowing model was presented. The different coefficients of the model, computed from both the measurements and the ray-tracing simulations, can be used to characterize the areas shadowed by a truck inside a 4-lane road scenario.

Acknowledgment

The authors would like to thank Køreteknisk Anlæg Nørresundby for providing access to the area and the truck. The authors would also like to express their gratitude to Kristian Bank, Assistant Engineer from the Department of Electronics Systems, Aalborg University, for his effort and support with the measurement setup. This work was supported by Innovation Fund Denmark.

References

[1] G. Pocovi *et al.*, "Automation for On-road Vehicles: Use Cases and Requirements for Radio Design", *IEEE Vehicular Technology Conference (VTC Fall)*, 2015.

[2] W. Viriyasitavat *et al.*, "Vehicular Communications: Survey and Challenges of Channel and Propagation Models", *IEEE Vehicular Technology Magazine*, vol. 10, no. 2, pp. 55-66, June 2015.

[3] H. Ruisi *et al.*,"Vehicle-to-Vehicle Propagation Models With Large Vehicle Obstructions", *IEEE Transactions on Intelligent Transportation Systems*, vol. 15, no. 5, October 2014.

[4] R. Meireles *et al.*, "Experimental study on the impact of vehicular obstructions in VANETs", *IEEE Vehicular Networking Conference*, December 2010.

[5] A. Chelli *et al.*, "A Vehicle-to-Infrastructure Channel Model for Blind Corner Scattering Environments", *IEEE Vehicular Technology Conference (VTC Fall)*, 2013.

[6] G. Acosta-Marum, and M. A. Ingram,"Six Time- and Frequency-Selective Empirical Channel Models for Vehicular Wireless LANs", *IEEE Vehicular Technology Magazine*, vol. 2, no. 4, pp 4-11, December 2007.

[7] J. Gozalvez, *et al.*, "IEEE 802.11p Vehicle to Infrastructure Communications in Urban Environments", *IEEE Communications Magazine*, vol. 50, no. 5, pp. 176-183, May 2012.

[8] C. F. Mecklenbrauker, *et al.*, "Vehicular Channel Characterization and Its Implications for Wireless System Design and Performance", *Proceedings of the IEEE*, vol. 99, no. 7, pp. 1189-1212, July 2011.

[9] D. Matolak,"V2V Communication Channels: State of Knowledge, New Results, and What's Next", in *Communication Technologies for Vehicles, Lecture Notes in Computer Science*, Springer Berlin Heidelberg, vol. 7865, 2013.

[10] K. Dar *et al.*, "Wireless Communication Technologies for ITS Applications", *IEEE Communications Magazine*, vol. 48 , no. 5, pp. 156-162, May 2010.

[11] F. C. M. Wegman, and M. Slop, "Safety Effects of Road Design Standards in Europe", *The European Market for Infrastructural Projects*, September 1996.

[12] The International Council on Green Transportation, "European Vehicle Market Statistics", Pocketbook, 2014.

[13] AWE Communications, "Wave propagation and Radio Network Planning", http://www.awe-communications.com/, [Online; accessed February 2016]

[14] W. C. Y. Lee, *Mobile Communications Engineering*, 2nd Edition, McGraw Hill, 1983.